

# A Network of Field-Calibrated Low-Cost Sensor Measurements of PM<sub>2.5</sub> in Lomé, Togo, Over One to Two Years

Garima Raheja, Kokou Sabi, Hèzouwè Sonla, Eric Kokou Gbedjangni, Celeste M. McFarlane, Collins Gameli Hodoli, and Daniel M. Westervelt\*



Cite This: *ACS Earth Space Chem.* 2022, 6, 1011–1021



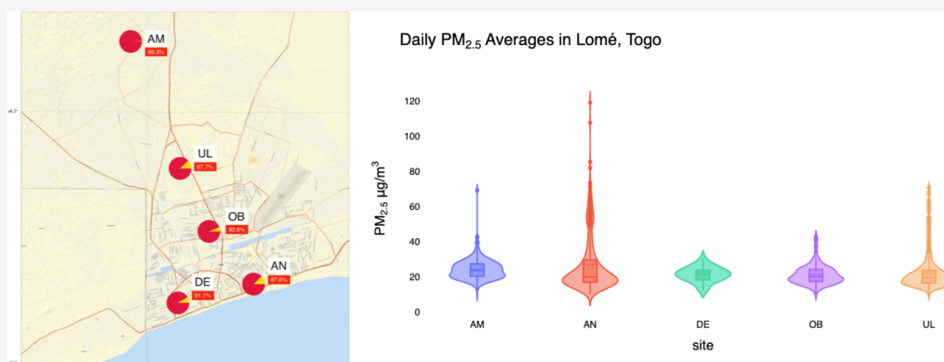
Read Online

ACCESS |

Metrics & More

Article Recommendations

Supporting Information



**ABSTRACT:** Air pollution is a leading cause of global premature mortality and is especially prevalent in many low- and middle-income countries (LMICs). In sub-Saharan Africa, preliminary monitoring networks, satellite retrievals of air-quality-relevant species, and air quality models show ambient fine particulate matter (PM<sub>2.5</sub>) concentrations that far exceed the World Health Organization guidelines, yet many areas remain largely unmonitored and understudied. Deploying a network of five low-cost PurpleAir PM<sub>2.5</sub> monitors over 2 years (2019–2021), we present the first multiyear ambient air pollution monitoring data results from Lomé, Togo, a major West African coastal city with a population of about 1.4 million people. The full-study time period network-wide mean measured daily PM<sub>2.5</sub> concentration is 23.5  $\mu\text{g m}^{-3}$ . The strong regional influence of the dry and dusty Harmattan wind increases the local average PM<sub>2.5</sub> concentration by up to 58% during December through February, but the diurnal and weekly trends in PM<sub>2.5</sub> are largely controlled by local influences. At all sites, more than 87% of measured days exceeded the new WHO Daily PM<sub>2.5</sub> guidelines; these first measurements highlight the need for air quality improvement in a rapidly growing urban metropolis.

**KEYWORDS:** air pollution, low-cost sensors, Africa, particulate matter, Harmattan

## 1. INTRODUCTION

Air pollution is a burgeoning global health crisis. In 2019, it rose from the fifth to the fourth leading risk factor for premature death, associated with 6.67 million premature deaths<sup>1</sup> and up to 6 million premature births.<sup>2</sup> Exposure to PM<sub>2.5</sub>, which is a form of air pollution composed of inhalable particulate matter smaller than 2.5  $\mu\text{m}$  in aerodynamic diameter, is linked to asthma, ischemic heart disease, type II diabetes, lung cancer, and other deleterious health effects.<sup>1</sup> These particles are emitted from vehicles, coal-burning power plants, waste incineration, and other anthropogenic and natural sources.<sup>1</sup> Thus far, most academic research, monitoring, and media attention regarding PM<sub>2.5</sub> exposure have been largely focused on the United States, Europe, and recently, China.<sup>3,4</sup> Additional research is vital and urgent for other regions where air pollution levels might be even higher.

In particular, countries in Asia, Africa, and the Middle East face the highest levels of ambient PM<sub>2.5</sub>.<sup>1,5</sup> Over the past

decade, regions in sub-Saharan Africa have seen drastic increases in PM<sub>2.5</sub> concentrations, while high-income countries in Europe and North America have seen steady declines.<sup>1,6</sup> Recent research shows that 1.1 million premature deaths were attributable to air pollution across the African continent in 2019;<sup>7</sup> in the same year, over 8000 premature deaths were attributed to air pollution in Togo, a West African nation with a population of 8.3 million.<sup>8</sup> These deaths are coupled with hundreds of thousands more cumulatively in neighboring West African countries including Nigeria and Ghana.<sup>8,9</sup> Diseases attributable to chronic air pollution exposure in a small handful

Received: November 11, 2021

Revised: February 18, 2022

Accepted: February 23, 2022

Published: March 10, 2022



Table 1. Sampling Locations, Durations, and Data Retrieval

#	site name	site code	location (latitude, longitude)	duration	number of days of data retrieved
1	Office du Bac	OB	6.152, 1.224	01-23-2020 to 05-10-2021	241
2	Direction de l'Environnement	DE	6.125, 1.212	01-20-2020 to 04-19-2021	34
3	Université de Lomé	UL	6.177, 1.212	07-10-2019 to 06-30-2021	695
4	Agoè Minamadou	AM	6.227, 1.193	01-02-2018 to 06-30-2021	412
5	Agence Nationale de Gestion de l'Environnement	AN	6.132, 1.242	05-15-2019 to 08-13-2020	307

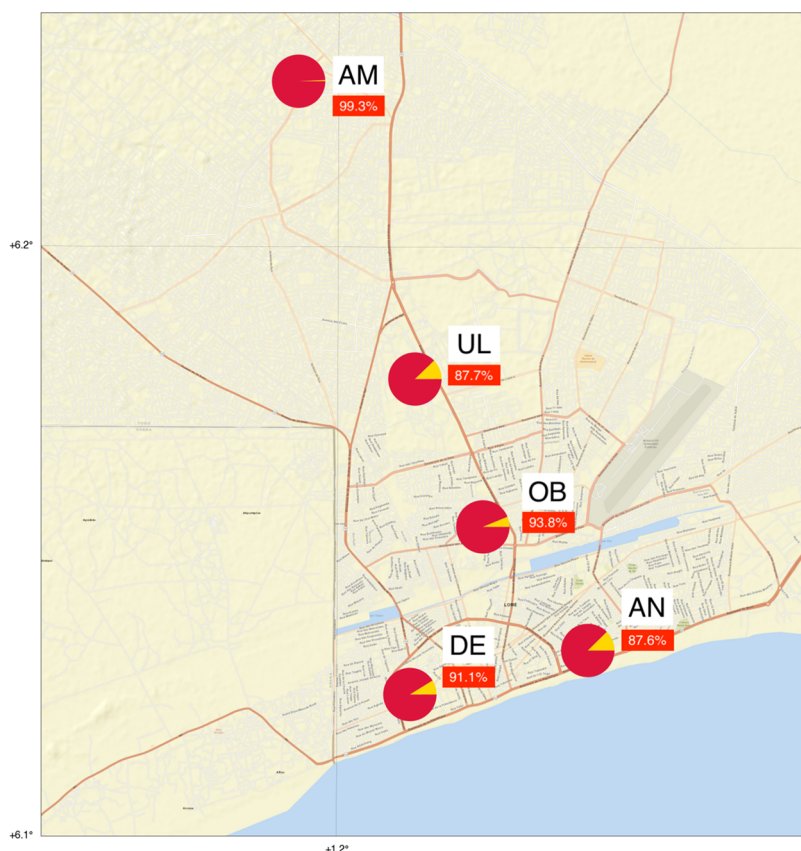


**Figure 1.** Network map and site-specific percent of measured days exceeding WHO daily  $PM_{2.5}$  guideline ( $15 \mu g m^{-3}$ ). The five sites are located at the Office du Bac (OB), Direction de l'Environnement (DE), Université de Lomé (UL), Agoè Minamadou (AM), and Agence Nationale de Gestion de l'Environnement (AN). Each pie represents the percentage of measured days exceeding WHO Daily  $PM_{2.5}$  Guideline ( $15 \mu g m^{-3}$ ).

of West African countries lead to a cumulative loss of over 5 million years of healthy life.<sup>10</sup>

However, these estimated health impact numbers are extremely uncertain and preliminary in areas where neither air quality nor public health data are available. While in Europe and the United States, the mean population distance of a person to a  $PM_{2.5}$  monitor is approximately 0–50 km, the global mean population distance of a person to a  $PM_{2.5}$  monitor is about 220 km.<sup>3</sup> This metric is largely influenced by the sparsity of monitors in low- and middle-income countries (LMICs).<sup>3</sup> Throughout the entire African continent, approximately 400 million children live in areas with no reliable air quality monitoring, making actual impacts uncertain.<sup>11</sup> Often, this sparsity in air pollution monitoring is engendered by the high cost of equipment; Federal Equivalent Method or Federal Reference Method equipment (referred to as reference monitors), which measure ambient  $PM_{2.5}$  concentrations, such as the frequently used Met One Beta Attenuation Monitor (BAM) 1020 or Teledyne T640, can cost several hundreds of thousands of dollars, including instrument

climate control, power needs, and associated maintenance costs. Even when a city or regional agency accrues the funds to purchase a monitor, the singular monitor cannot capture the vast heterogeneity that has been shown to impact neighborhood-scale exposure.<sup>12,13</sup>

Recent advances in low-cost sensor (LCS) measurement technology, and calibration of low-cost sensor data using data science techniques, allow for high-density, real-time monitoring, and automated web-based archiving of ambient  $PM_{2.5}$  concentrations. LCS for measuring air pollution and identifying sources offer a possible path forward to remedy the lack of data in resource-limited locations such as sub-Saharan Africa. For LCS to provide useful, actionable information, understanding local conditions is vital. Calibration factors and sensor technical performance vary strongly with particle optical properties, which are influenced by size, composition, and loading (Mie Theory), as well as environmental conditions affecting hygroscopicity, such as temperature and humidity. The PurpleAir monitor, when calibrated

and corrected correctly, has demonstrated high accuracy in comparison to reference-grade monitors.<sup>14–18</sup>

In 2014, Togo joined the Climate and Clean Air Coalition, and in 2020, it adopted a National Plan for the Reduction of Air Pollution and Short-Lived Climate Pollutants “which will reap the multiple benefits of improving air quality, fighting climate change, and realizing co-benefits like improved health and agricultural productivity. Fully implementing it will result in a 67 percent reduction in black carbon, a 70 percent reduction in fine particulate matter, and a 56 percent methane reduction by 2040”.<sup>8</sup> However, to quantify reductions, it is vital to have measurements. The proposed PM<sub>2.5</sub> reductions in the National Plan require a well-calibrated and distributed network of measurements at present to establish a baseline for estimating the impact of air pollution mitigation.

To our knowledge, there are no published ambient PM<sub>2.5</sub> measurement data in the country of Togo. Amouzouvi et al.<sup>19</sup> simulated PM, SO<sub>2</sub>, and NO<sub>2</sub> in Lomé using the USEPA AERMOD dispersion model, but no ground-based observational data were included in the study. Diallo et al.<sup>20</sup> measured personal exposure to PM<sub>2.5</sub> in Lomé indoor environments using simple devices. The DACCIWA project included plane flights over the Lomé airspace and included chemical sampling.<sup>21</sup> However, none of these studies have included long-term stationary surface observations of PM<sub>2.5</sub>, which are critical for future health and pollution studies.

Here, we present the first-ever multiyear field-calibrated PM<sub>2.5</sub> dataset in Lomé, the capital city of Togo, a major coastal city in West Africa with a metropolitan population of 1.4 million. Lomé was also expected to grow by 5.3% in 2021,<sup>22</sup> indicating a need to address air quality issues early as the city expands. We deployed a network of five PurpleAir monitors starting in late 2019 and used Gaussian mixture regression-based correction factors. McFarlane et al.<sup>14,27</sup> developed through a year-long field calibration with a federal equivalent method (FEM) a PM<sub>2.5</sub> instrument in neighboring Accra, Ghana (approximately 190 km due west of Lomé), to analyze PM<sub>2.5</sub> on annual, monthly, weekly, daily, and hourly timescales. Finally, we assess the relative ambient air pollution levels in comparison to global air quality guidelines from the World Health Organization.

## 2. METHODS

**2.1. Description of PurpleAir Sensors.** We deploy five PurpleAir monitors around Lomé, Togo. The monitors are commercially available and cost approximately USD \$250 each. Each monitor contains dual Plantower PMS5003 light scattering sensors to estimate PM<sub>2.5</sub> mass concentrations and one Bosch BME 280 sensor to estimate pressure, relative humidity, and temperature.<sup>23</sup> The Plantower sensors sample at approximately 1 min frequency. When correction factors are applied to raw sensor data, PM<sub>2.5</sub> concentrations reported by PMS5003 sensors have been known to correlate strongly with PM<sub>2.5</sub> concentrations reported by reference-grade monitors.<sup>18,24–26</sup> We convert the raw PurpleAir outputs using the<sup>27</sup> Gaussian mixture regression model-based correction, described in Section 2.3, and then average the corrected output to hourly, daily, and annual timescales for analysis.

**2.2. Sampling Locations and Periods.** PurpleAir monitors were placed at five sites, as listed in Table 1 and mapped in Figure 1. Though the total sampling period to date amounts to approximately 2 years, multiple monitors had data logging issues due to WiFi connectivity issues. In particular, the

Direction de l'Environnement (DE) site was severely impacted, with only 34 days of data retrieved. The ensuing analysis therefore focuses on the other four locations (OB, UL, AM, AN) though DE is included where possible. Table 1 lists the site names, exact locations, and duration of data collection.

**2.3. Calibration and Correction.** First, we apply standard quality assurance and quality control on the raw PurpleAir data, removing data points containing NaN values, negative values, PM<sub>2.5</sub> values outside the optimal PurpleAir measurement range (below 0  $\mu\text{g m}^{-3}$  and above 1000  $\mu\text{g m}^{-3}$ ), and where the Channel A and Channel B measurements differ by greater than 20  $\mu\text{g m}^{-3}$ . Further, we remove data points where humidity measurements are greater than 100%. Table S1 lists the number of data points in each site removed in each cleaning step.

The Plantower sensors inside the PurpleAir monitors measure the scattering of light by particles and then convert the electrical signal into an ambient PM<sub>2.5</sub> concentration using a proprietary calibration algorithm.<sup>23</sup> However, the relationship between the light scattering signal measured by the sensor and the true PM<sub>2.5</sub> concentration is affected by the size distribution, shape, refractive index, and density of the particles being measured. Because these particle properties vary in real-world settings, in situ calibration and correction models are often developed and applied to improve the accuracy of PM<sub>2.5</sub> concentrations reported by PMS5003 sensors.<sup>15,28–31</sup>

PurpleAir-reported PM<sub>2.5</sub> concentrations are generally corrected by co-locating a reference-grade monitor with a PurpleAir monitor at the same site and then creating various forms of regression-based corrections of differing complexities. However, currently, there are no reference-grade PM<sub>2.5</sub> monitors in Togo. Previous research has shown that low-cost sensors' (such as PurpleAir) output values can be highly accurate in regard to reference-grade monitors when they are corrected to account for temperature and relative humidity.<sup>15,28–32</sup> This implies that correction factors are transferable within a region with approximately homogeneous climatology and aerosol size, composition, and loading.

Given the largely similar climatology in weather and aerosol quantities between Lomé and Accra, in this study, we correct values from the PurpleAir monitors in Lomé using the Gaussian mixture regression (GMR) correction factor scheme developed by McFarlane et al.<sup>27</sup> who colocated a PurpleAir monitor with a Met One BAM 1020 monitor in Accra. Briefly, GMR works by modeling the probability density of the output data conditional to the input data as a Gaussian mixture model, allowing it to capture complex, nonlinear relationships and handle missing data from explanatory variables. Thus, GMR models have demonstrated better R<sup>2</sup> and mean absolute error in comparison to the more commonly used multiple linear regression and random forest models in nearby Accra, Ghana.<sup>27</sup> The GMR model developed for Accra uses the raw PurpleAir PM<sub>2.5</sub> concentration, the temperature measured inside the PurpleAir monitor, and the relative humidity measured inside the PurpleAir monitor to predict the corrected PM<sub>2.5</sub> concentration. Lomé is approximately 190 km due east of Accra, and the two cities have similar climatology. Our approach also assumes that Lomé and Accra experience PM<sub>2.5</sub> pollution from similar sources and thus with a similar range of compositions. Up to date information on sources of PM<sub>2.5</sub> are severely lacking in Africa, but we use the DICE-Africa emissions inventory<sup>33</sup> to assess the similarity of sources of SO<sub>2</sub>, black carbon (BC), and organic carbon (OC) in both

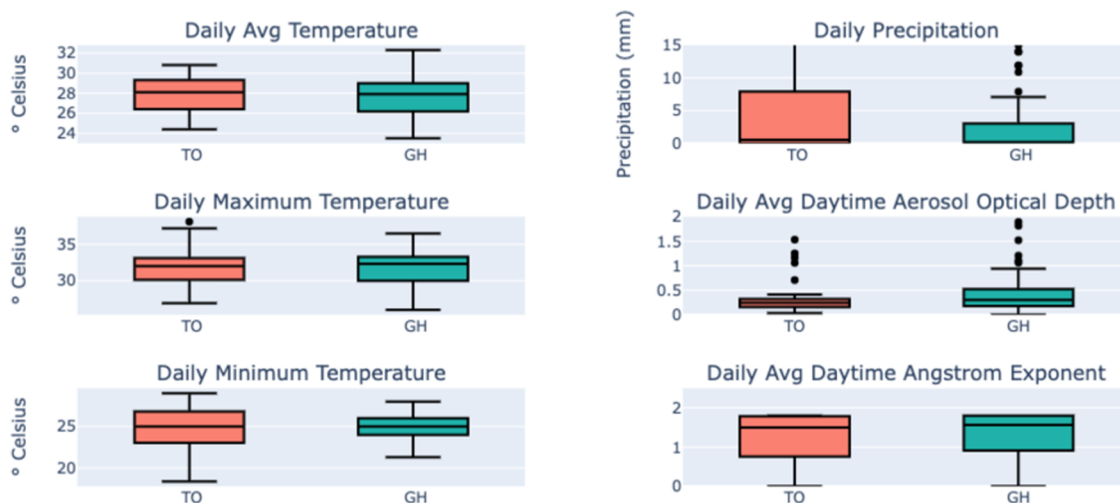


**Figure 2.** Climatology comparison between Lomé, Togo, and Accra, Ghana for 11/2018–11/2020 (Note: Ångström exponent distribution is from 11/2019–11/2020).

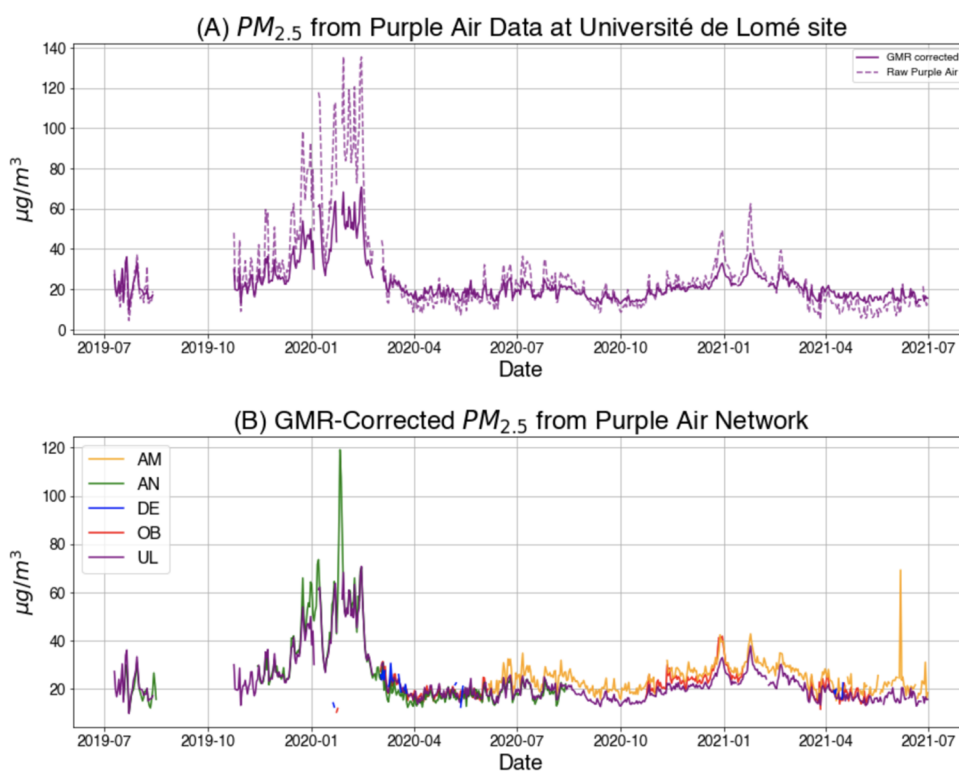


**Figure 3.** (A) Raw vs Accra-based Gaussian mixture regression correction. (B) Corrected  $PM_{2.5}$  from Lomé PurpleAir Network.

cities. Figure S2 shows that the source mix between the two cities for these two pollutants is quite similar, with cars being the dominant source of  $SO_2$ , cars and motorcycles the dominant source of OC, and household fuelwood and kerosene use the dominant source of BC in both Accra and Lomé.

Figure 2 compares the distributions of daily average temperature, daily maximum temperature, daily minimum temperature, and daily precipitation from November 1, 2018, to November 1, 2020, in Lomé, Togo, and Accra, Ghana. Figure S1 also compares Multi-Angle Implementation of Atmospheric Correction (MAIAC) algorithm-based Level-2 gridded (L2G) aerosol optical depth (AOD) at  $0.55 \mu\text{m}$  and MODIS Aqua Deep Blue Ångström Exponent in the two cities

during the same time period. Temperature and precipitation measurements from measurement stations at Gnassingbé Eyadéma International airport in Lomé and Kotoka International Airport in Accra are taken from the National Oceanic and Atmospheric Administration's National Centers for Environmental Information Climate Data Online Portal ([www.ncdc.noaa.gov/cdo-web/](http://www.ncdc.noaa.gov/cdo-web/)). AOD and Ångström exponent measurements are extracted from MCD19A2 MODIS Terra and Aqua MODIS 1 km resolution L2 products and MYD08\_D3 MODIS Aqua  $1 \times 1$  degree grid L3 products, respectively. These products are provided by the National Aeronautics and Space Administration's Atmosphere Archive & Distribution System Distributed Active Archive Center

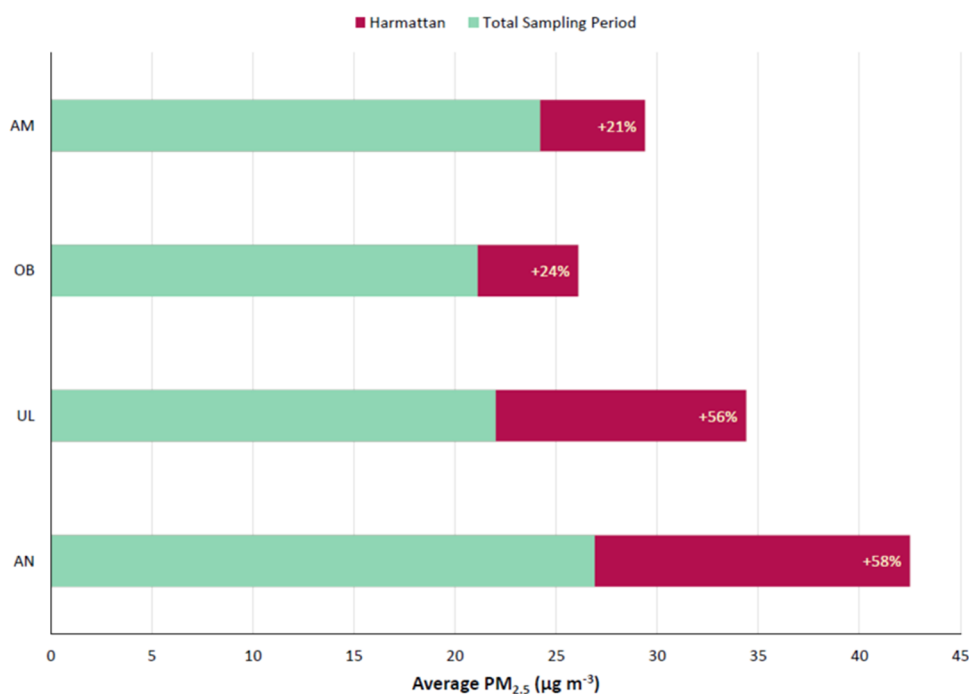


**Figure 4.** Harmattan enhancements in average  $\text{PM}_{2.5}$  at five sites. The green bar is the average  $\text{PM}_{2.5}$  concentration at the site over the full sampling period. The sum of the green bar and the red bar is the average  $\text{PM}_{2.5}$  concentration at the site during the Harmattan (December–February). The text inside each red bar indicates how much higher the average  $\text{PM}_{2.5}$  concentration during the Harmattan was compared to the average  $\text{PM}_{2.5}$  concentration over the 2-year sampling period.

(NASA LAADS DAAC) at latitude, longitude coordinates of 6.136, 1.222 for Lomé and 5.615,  $-0.203$  for Accra.

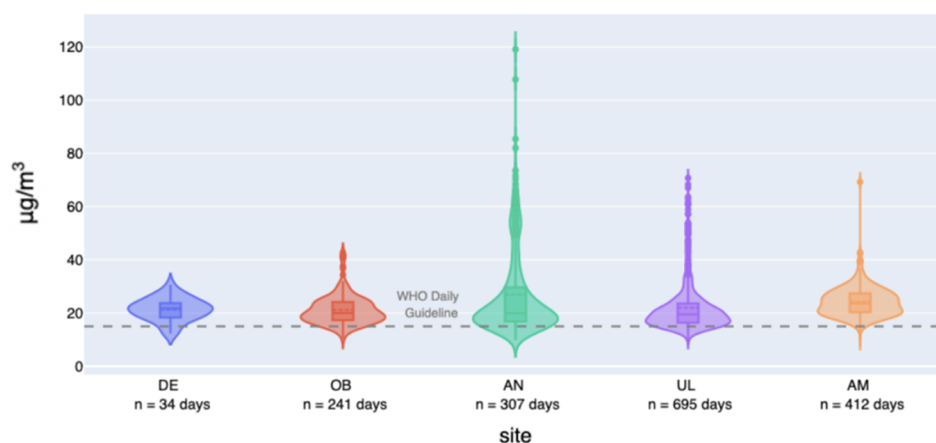
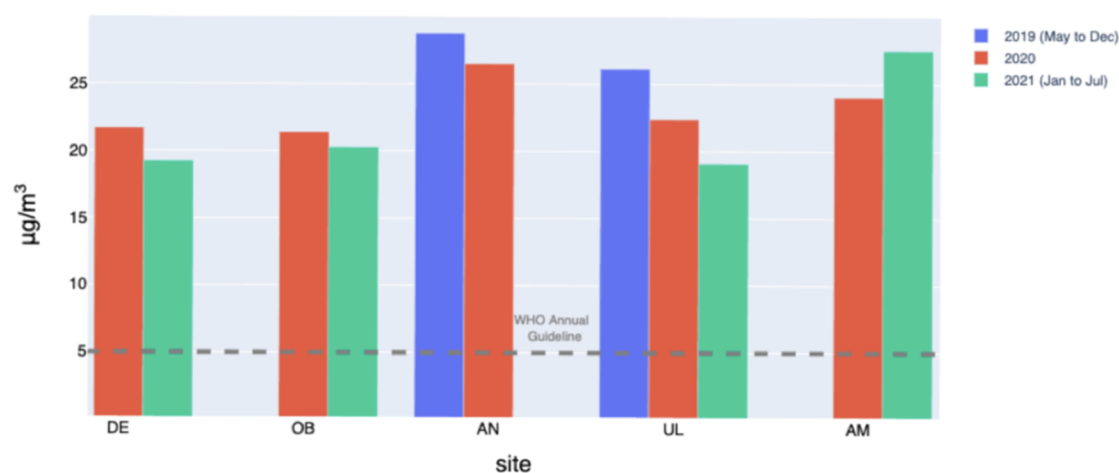
Temperatures in Lomé, Togo, and Accra, Ghana, compare closely. Mean daily average temperatures are 27.9 and 27.7 °C, mean daily maximum temperatures are 31.6 and 31.7 °C, and mean daily minimum temperatures are 24.8 and 24.9 °C, respectively. Precipitation, aerosol optical depths, and Ångström exponents within the two cities are also similar (Figure 2), which indicates some qualitative consistency in average particle size in both locations.<sup>34</sup> The mean Ångström exponent is 1.19 in Lomé and 1.31 in Accra, indicating an average mix of combustion-sized aerosols and larger dust-sized aerosols. The mean daily precipitation is 6.7 and 5.1 mm, the mean observed aerosol optical depths are 0.37 and 0.45, and the mean observed Ångström exponents are 1.19 and 1.32 in Lomé, Togo, and Accra, Ghana, respectively. (The precipitation distribution is shown solely as a boxplot for clarity to demonstrate the low average and high tail.) We note that both Accra, where the calibration was developed, and Lomé, are heavily impacted by the dust from the Harmattan season, which resulted in both the highest raw and corrected  $\text{PM}_{2.5}$  values during the measurement period. McFarlane et al.,<sup>14,27</sup> who developed the correction factor, found that the raw PurpleAir output sometimes underestimated the highest peak of  $\text{PM}_{2.5}$  during Harmattan, but that the correction factor reduced this bias to around zero, giving us confidence that the method can accurately diagnose these high- $\text{PM}_{2.5}$  events.<sup>27</sup>

### 3. RESULTS

Figure 3A shows a largely continuous daily average raw PurpleAir data time series (red line) and the corresponding GMR-corrected time series (yellow line) at the Université de Lomé site. The time series spans July 2019 to July 2021; there is a brief interruption in data logging around September 2019

due to power interruptions. The GMR-corrected time series exhibits highly similar temporal patterns but generally reduces concentrations during peak concentration times, consistent with previous findings that PurpleAir monitors tend to overpredict  $\text{PM}_{2.5}$  concentrations.<sup>15</sup> The largest peaks in both raw and corrected concentrations occur during the Harmattan season in West Africa, occurring from around December to February. During non-Harmattan, raw and corrected PurpleAir  $\text{PM}_{2.5}$  concentrations are very similar. Elevated  $\text{PM}_{2.5}$  concentrations are expected during this time since the Harmattan is a dry, dusty northeasterly wind that blows dust from the Sahara desert over West Africa.

In Figure 3B, we use the same GMR correction demonstrated in Figure 3A and apply it to all of the sites in the network. This allows for comparison and contrast at all sites, showing that the AN and AM sites exhibit the highest concentrations during their respective measurement periods. The AN site is located in a downtown area next to a major highway, which could explain elevated anthropogenic aerosols. The AN site is also near the coastline, which could indicate sea salt aerosol influence. Peak daily mean concentrations at AN reach nearly 120  $\mu\text{g m}^{-3}$ , indicating an extreme air quality event. Though this peak occurs during the middle of the Harmattan season, the Harmattan is unlikely to explain the large  $\text{PM}_{2.5}$  enhancement since the Harmattan is a large-scale regional phenomenon and the large peak is not present at the other sampling sites within the network. The AM site is farthest inland and in a residential neighborhood with unpaved dirt roads and frequent waste burning by local residents; thus, the elevated concentrations could be explained by a combination of waste burning and dust. Data collected on waste burning in the neighborhood surrounding the AM site indicate high fractions of organic waste and fines.<sup>35</sup>

(A) GMR-Corrected Distribution of Daily PM<sub>2.5</sub> Averages(B) GMR-Corrected Annual PM<sub>2.5</sub> Averages

**Figure 5.** (A) GMR-corrected distribution of daily PM<sub>2.5</sub> averages at five sites. (B) GMR-corrected distribution of annual PM<sub>2.5</sub> averages at five sites.

We also find that the enhancement in concentrations during the December 2019 to February 2020 Harmattan period is much higher than the enhancement during the December 2020 to February 2021 Harmattan period. Figure 4 is created by averaging the daily PM<sub>2.5</sub> concentrations over the full 2-year period and then separately during the Harmattan (defined as December 1 to February 28), and shows that the sites have Harmattan PM<sub>2.5</sub> averages that are 21–58% higher compared to their respective total sampling period averages. The lowest concentrations at each site generally occur in April–May during the first and strongest rainy season, and then again in September–October when the Intertropical Convergence Zone (ITCZ) retreats back toward the south. The seasonality of the PM<sub>2.5</sub> concentrations at each site generally follows the precipitation and Harmattan seasonal patterns.

Figure 5A shows the GMR-corrected distributions of daily PM<sub>2.5</sub> averages at all of the sites, with the 2021 WHO Daily PM<sub>2.5</sub> Guideline ( $15 \mu\text{g m}^{-3}$ ) plotted in a gray dashed line. All sites have mean daily concentrations above the WHO PM<sub>2.5</sub> Guideline. The AN site has a particularly long tail, possibly due to the influence of dense urban traffic emissions on certain

days. Though each site has a different number of daily samples (Figure 5A), making exact intercomparisons between sites not straightforward, the concentrations are mostly homogeneous throughout the five sites. Figure 5B illustrates the annual PM<sub>2.5</sub> averages for all of the sites. Note that the 2019 and 2021 sampling periods are incomplete years. All sites consistently see annual averages 4–5 times greater than the 2021 WHO Annual Guideline ( $5 \mu\text{g m}^{-3}$ ). Though an incomplete year, 2021 (January through July) has a much weaker Harmattan with lower PM<sub>2.5</sub> concentrations (see Figure 3B), which can likely explain the drop-off in PM<sub>2.5</sub> at each of the sites compared to 2020.

Figure 6 compares the diurnal cycle during Harmattan (December/January/February) and non-Harmattan times at four of the five sites (DE was not included due to a dearth of available data). The hourly averages are plotted; for reference, the concentrations above the WHO Daily Guideline are shaded in red and the concentrations below the guideline are shaded in green. All four sites demonstrate a strong morning time peak (5–8 AM) and a slight evening time peak. The morning and evening peaks could be a combination of cooking

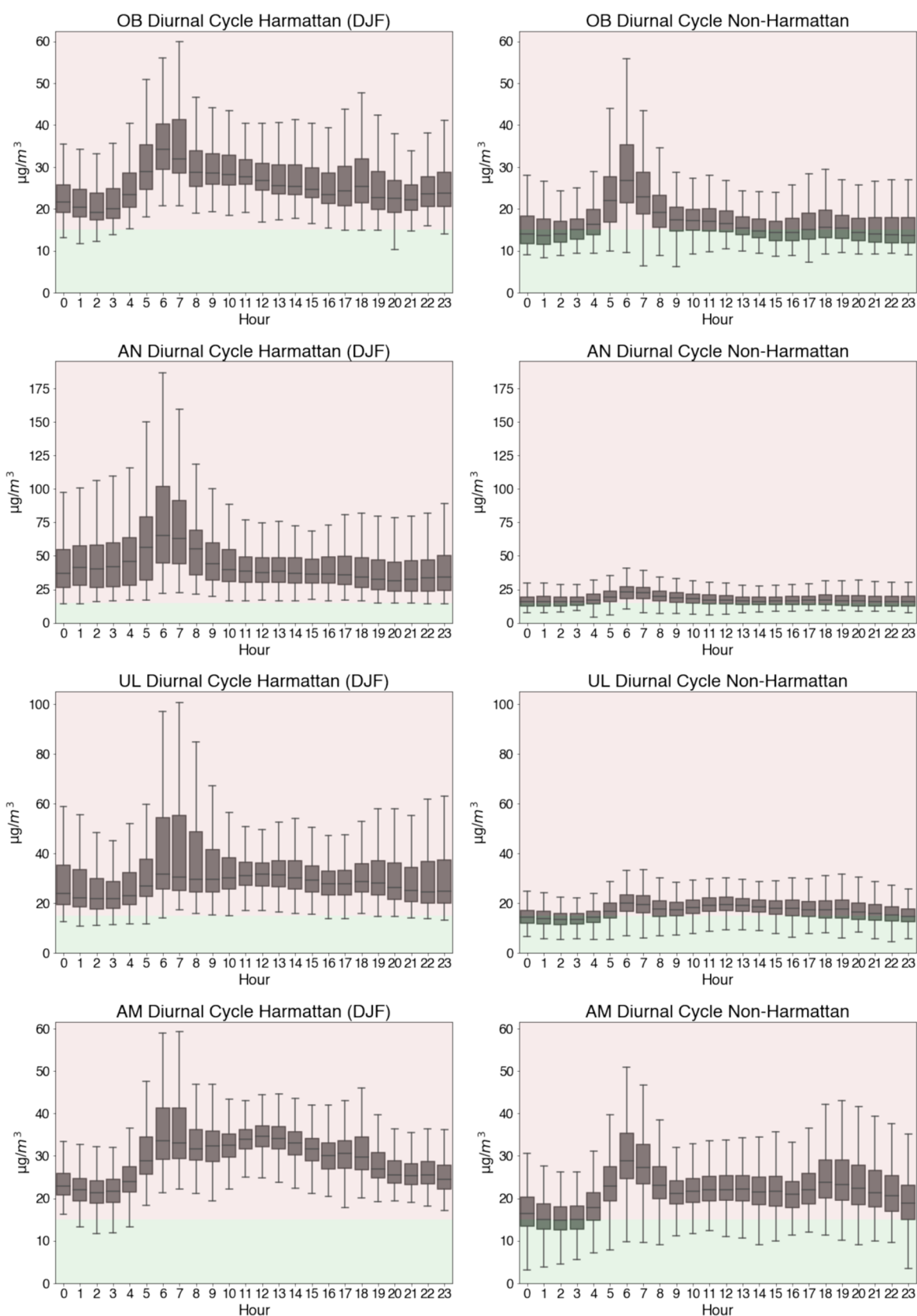


**Figure 6.** Site-specific diurnal cycles during Harmattan (DJF = December–January–February) and non-Harmattan (March–November) periods.

emissions and rush hour traffic emissions (both through fuel combustion and suspension of dust on unpaved roads), and local waste burning, which occurs frequently at the AM site as described previously. Out of all of the sites, Harmattan and

non-Harmattan  $\text{PM}_{2.5}$  concentration magnitudes and diurnal cycles are most consistent at the AM site, suggesting that this site might be most sensitive to local pollution influences (e.g., waste burning) and least sensitive to Harmattan elevations. In

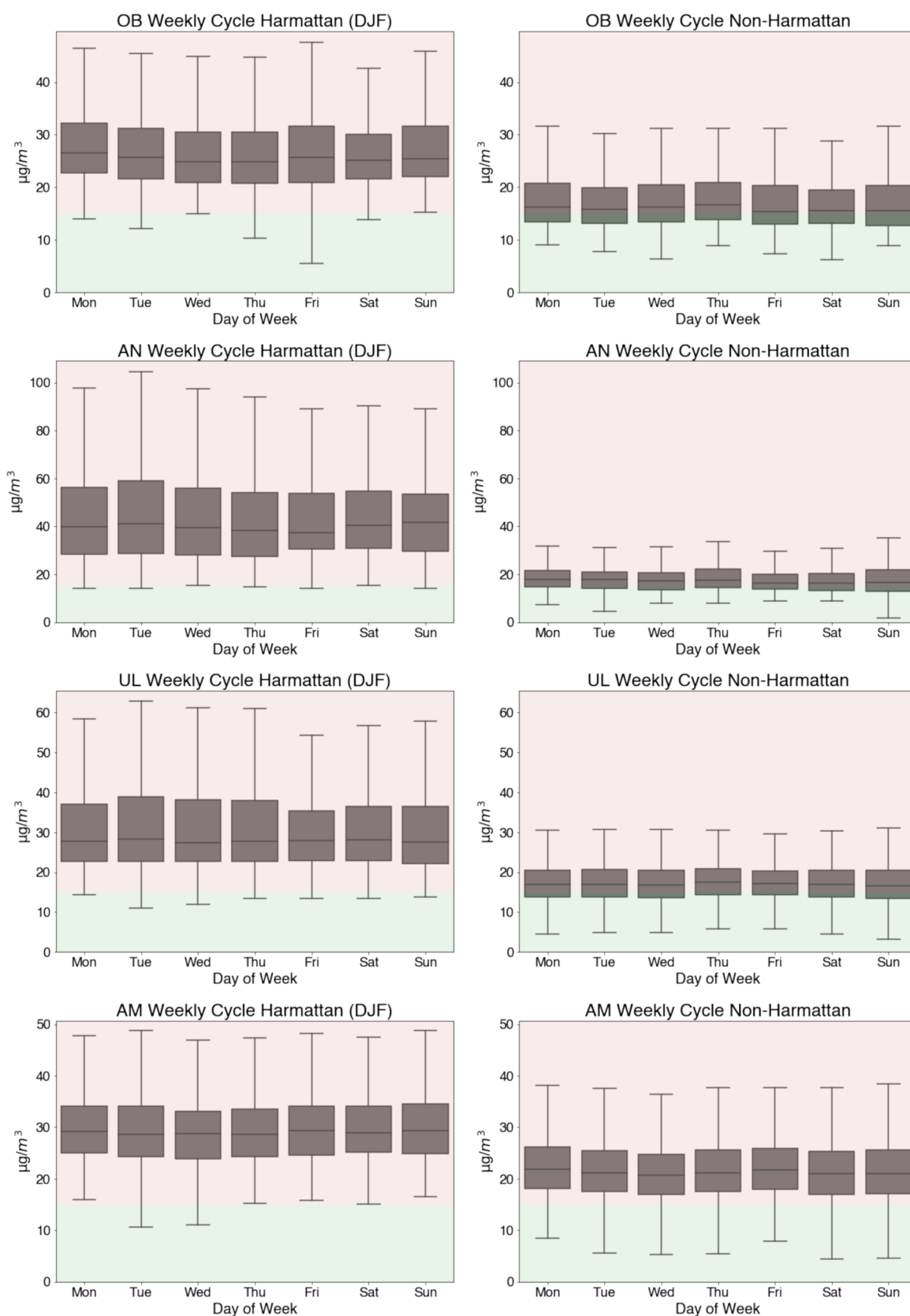


**Figure 7.** Site-specific weekly cycles during Harmattan (DJF = December–January–February) and non-Harmattan (March–November) periods.

contrast, at the three sites closest to the city center, the baselines of the diurnal cycles and therefore the total concentrations during the Harmattan are drastically elevated, indicating a big regional influence. The average hourly PM<sub>2.5</sub>

concentrations at 6:00 AM from March to November are 20.3 µg m<sup>-3</sup> (UL), 23.5 µg m<sup>-3</sup> (AN), 29.5 µg m<sup>-3</sup> (OB), and 31.3 µg m<sup>-3</sup> (AM). In contrast, the average hourly PM<sub>2.5</sub> concentrations at 6:00 AM during the Harmattan are 41.6



$\mu\text{g m}^{-3}$  (UL),  $75.9 \mu\text{g m}^{-3}$  (AN),  $35.2 \mu\text{g m}^{-3}$  (OB), and  $37.5 \mu\text{g m}^{-3}$  (AM).

Figure 7 compares the weekly cycle during Harmattan and non-Harmattan times at four sites. All four sites demonstrate almost consistent weekly cycles, with little drop-off over the weekends; all four sites also show clear elevated levels of  $\text{PM}_{2.5}$  during the Harmattan period. Notably, during the Harmattan, it is rare for concentrations to dip below the WHO daily guideline (green shaded region), but outside of the Harmattan, this is significantly more common. From Figures 6 and 7, it is evident that the Harmattan appears to drive up baseline concentrations, but the diurnal and weekly patterns are largely dominated by local influences: for example, near the AM site, local collaborators have documented waste burning three to four times a week.

Revisiting Figure 1, at each site, we plot the percent of measured days exceeding the WHO Daily Guideline. At all sites, more than 87% of measured days exceeded the Guideline; at the AM site, 99.3% of measured days exceeded the Guideline. The WHO Daily Guideline was recently revised downward, but the concentrations in Lomé exceed the pre-2021 guideline 26% of the days as well. This emphasizes the importance of reducing local pollution sources in West African cities like Lomé, where a certain amount of baseline  $\text{PM}_{2.5}$  levels are essentially guaranteed by the Harmattan. While many cities around the world saw lowered  $\text{PM}_{2.5}$  concentrations during the COVID-19 lockdowns, in Lomé, the Harmattan may have overshadowed any potential improvements in  $\text{PM}_{2.5}$  concentrations due to lockdowns during 2020 (annual average  $21.3 \mu\text{g m}^{-3}$ ) compared to 2021 (annual average  $19.3 \mu\text{g m}^{-3}$ ), when lockdown restrictions were largely abandoned. This further emphasizes the need to craft strong mitigation policy that incorporates local and regional effects for major West African cities such as Lomé and also shows the importance of early warning systems and air quality forecasting to equip people with information that can help them reduce exposure to  $\text{PM}_{2.5}$  during intense Harmattan periods.

#### 4. CONCLUSIONS

We present the first observations of  $\text{PM}_{2.5}$  air pollution in Lomé, Togo, from 2 years of measurements derived from field-calibrated low-cost PurpleAir  $\text{PM}_{2.5}$  monitors. The network spans the urban core, coastal region, and the outer metropolis; at all measurement sites, more than 87% of measured days exceeded the newly released 2021 WHO Daily  $\text{PM}_{2.5}$  guideline (26% of measured days exceeded the pre-2021 WHO daily  $25 \mu\text{g m}^{-3}$  guideline). Togo does not yet have its own air quality monitoring standards. Network-wide average  $\text{PM}_{2.5}$  through the entire sampling period is  $23.2 \mu\text{g m}^{-3}$ . This is lower than Accra, Ghana ( $49.5 \mu\text{g m}^{-3}$ ), Abidjan, Côte d'Ivoire ( $23.8$ – $113.4 \mu\text{g m}^{-3}$ ), and Kasuwa, Nigeria ( $65 \mu\text{g m}^{-3}$ ), indicating that while air quality is at unhealthy levels in Togo, it may not be as severe as several other West and Central African cities.<sup>36–38</sup> Though the trends at subannual timescales are driven by local patterns, the baseline levels are heavily elevated by the Harmattan, which increases  $\text{PM}_{2.5}$  concentrations by 21–56% in December, January, and February. Continued measurements of  $\text{PM}_{2.5}$  and potentially gas-phase pollutants at these five sites as well as new planned sites will help understand the distribution of pollution in the growing city and how they are affected by natural and anthropogenic variations. Further study could also aim to understand sensor aging and drift, quantify health impacts such as morbidity and

mortality rates in this region, and suggest methods for policy-driven reductions in pollution concentrations.

#### ■ ASSOCIATED CONTENT

##### Supporting Information

The Supporting Information is available free of charge at <https://pubs.acs.org/doi/10.1021/acsearthspacechem.1c00391>.

Data cleaning: number of data points remaining after each step of data cleaning (Table S1); time-averaged map of aerosol optical depth 550 nm (Figure S1); and relative contributions of source sectors to pollutant emissions in Lomé, Togo, from DICE-Africa 2013 Inventory (Figure S2) (PDF)

#### ■ AUTHOR INFORMATION

##### Corresponding Author

Daniel M. Westervelt – Lamont-Doherty Earth Observatory of Columbia University, Palisades, New York 10964, United States; NASA Goddard Institute for Space Studies, New York, New York 10025, United States; [orcid.org/0000-0003-0806-9961](https://orcid.org/0000-0003-0806-9961); Email: [danielmw@ldeo.columbia.edu](mailto:danielmw@ldeo.columbia.edu)

##### Authors

Garima Raheja – Lamont-Doherty Earth Observatory of Columbia University, Palisades, New York 10964, United States; Department of Earth and Environmental Science, Columbia University, New York, New York 10027, United States; [orcid.org/0000-0002-5037-7979](https://orcid.org/0000-0002-5037-7979)

Kokou Sabi – Université de Lomé (UL), 1515 Lomé, Togo  
Hézuwè Sonla – Université de Lomé (UL), 1515 Lomé, Togo

Eric Kokou Gbedjangni – Université de Lomé (UL), 1515 Lomé, Togo

Celeste M. McFarlane – Lamont-Doherty Earth Observatory of Columbia University, Palisades, New York 10964, United States; [orcid.org/0000-0003-2530-3051](https://orcid.org/0000-0003-2530-3051)

Collins Gameli Hodoli – Clean Air One Atmosphere, 3385 Tema, Accra, Ghana

Complete contact information is available at:

<https://pubs.acs.org/doi/10.1021/acsearthspacechem.1c00391>

##### Notes

The authors declare no competing financial interest.

#### ■ ACKNOWLEDGMENTS

The authors acknowledge funding from the US National Science Foundation (NSF) Grant Number OISE 2020677. They declare no conflict of interest. All data used in this study can be downloaded from purpleair.com. No unexpected or unusually high safety hazards were encountered during this study.

#### ■ REFERENCES

- (1) Health Effects Institute. *State of Global Air 2020, Special Report*. Health Effects Institute, 2020.
- (2) Ghosh, R.; Causey, K.; Burkart, K.; Wozniak, S.; Cohen, A.; Brauer, M. Ambient and Household  $\text{PM}_{2.5}$  Pollution and Adverse Perinatal Outcomes: A Meta-Regression and Analysis of Attributable Global Burden for 204 Countries and Territories. *PLoS Med.* **2021**, *18*, No. e1003718.
- (3) Martin, R. V.; Brauer, M.; van Donkelaar, A.; Shaddick, G.; Narain, U.; Dey, S. No One Knows Which City Has the Highest

- Concentration of Fine Particulate Matter. *Atmos. Environ.: X* **2019**, *3*, No. 100040.
- (4) Hasenkopf, C. A.; Veghte, D. P.; Schill, G. P.; Lodoysamba, S.; Freedman, M. A.; Tolbert, M. A. Ice Nucleation, Shape, and Composition of Aerosol Particles in One of the Most Polluted Cities in the World: Ulaanbaatar, Mongolia. *Atmos. Environ.* **2016**, *139*, 222–229.
- (5) Pirlea, F. WDI - The Global Distribution of Air Pollution. <https://datatopics.worldbank.org/world-development-indicators/stories/the-global-distribution-of-air-pollution.html> (accessed Oct 13, 2021).
- (6) Cohen, A. J.; Brauer, M.; Burnett, R.; Anderson, H. R.; Frostad, J.; Estep, K.; Balakrishnan, K.; Brunekreef, B.; Dandona, L.; Dandona, R.; Feigin, V.; Freedman, G.; Hubbell, B.; Jobling, A.; Kan, H.; Knibbs, L.; Liu, Y.; Martin, R.; Morawska, L.; Pope, C. A.; Shin, H.; Straif, K.; Shaddick, G.; Thomas, M.; van Dingenen, R.; van Donkelaar, A.; Vos, T.; Murray, C. J. L.; Forouzanfar, M. H. Estimates and 25-Year Trends of the Global Burden of Disease Attributable to Ambient Air Pollution: An Analysis of Data from the Global Burden of Diseases Study 2015. *Lancet* **2017**, *389*, 1907–1918.
- (7) Fisher, S.; Bellinger, D. C.; Cropper, M. L.; Kumar, P.; Binagwaho, A.; Koudenoukpo, J. B.; Park, Y.; Taghian, G.; Landrigan, P. J. Air Pollution and Development in Africa: Impacts on Health, the Economy, and Human Capital. *Lancet Planet Health* **2021**, *10*, e681–e688.
- (8) CCAC Secretariat. Togo's Minister of Environment endorses first National Plan to Reduce Air Pollutants and Short-Lived Climate Pollutants. <https://www.ccacoalition.org/en/news/togo%E2%80%99s-minister-environment-endorses-first-national-plan-reduce-air-pollutants-and-short-lived> (accessed Oct 13, 2021).
- (9) Bauer, S. E.; Im, U.; Mezuman, K.; Gao, C. Y. Desert Dust, Industrialization, and Agricultural Fires: Health Impacts of Outdoor Air Pollution in Africa. *J. Geophys. Res.: Atmos.* **2019**, *124*, 4104–4120.
- (10) GAHP. *Pollution and Health Metrics - Global, Regional and Country Analysis*; Global Alliance on Health and Pollution, Dec, 2019.
- (11) UNICEF. *Silent Suffocation in Africa Air Pollution Is a Growing Menace, Affecting the Poorest Children the Most*; United Nations Children's Fund, 2019.
- (12) Shusterman, A. A.; Teige, V. E.; Turner, A. J.; Newman, C.; Kim, J.; Cohen, R. C. The Berkeley Atmospheric CO<sub>2</sub> Observation Network: Initial Evaluation. *Atmos. Chem. Phys.* **2016**, *16*, 13449–13463.
- (13) Apte, J. S.; Messier, K. P.; Gani, S.; Brauer, M.; Kirchstetter, T. W.; Lunden, M. M.; Marshall, J. D.; Portier, C. J.; Vermeulen, R. C. H.; Hamburg, S. P. High-Resolution Air Pollution Mapping with Google Street View Cars: Exploiting Big Data. *Environ. Sci. Technol.* **2017**, *51*, 6999–7008.
- (14) McFarlane, C.; Isevulambire, P. K.; Lumbuenamo, R. S.; Ndinga, A. M. E.; Dhammapala, R.; Jin, X.; McNeill, V. F.; Malings, C.; Subramanian, R.; Westervelt, D. M. First Measurements of Ambient PM<sub>2.5</sub> in Kinshasa, Democratic Republic of Congo and Brazzaville, Republic of Congo Using Field-Calibrated Low-Cost Sensors. *Aerosol Air Qual. Res.* **2021**, *21*, 1–16.
- (15) Malings, C.; Tanzer, R.; Haurlyiuk, A.; Saha, P. K.; Robinson, A. L.; Presto, A. A.; Subramanian, R. Fine Particle Mass Monitoring with Low-Cost Sensors: Corrections and Long-Term Performance Evaluation. *Aerosol Sci. Technol.* **2020**, *54*, 160–174.
- (16) Ardon-Dryer, K.; Dryer, Y.; Williams, J. N.; Moghimi, N. Measurements of PM<sub>2.5</sub> with PurpleAir under Atmospheric Conditions. *Atmos. Meas. Tech.* **2020**, *13*, 5441–5458.
- (17) Stavroulas, I.; Grivas, G.; Michalopoulos, P.; Liakakou, E.; Bougiatioti, A.; Kalkavouras, P.; Fameli, K. M.; Hatzianastassiou, N.; Mihalopoulos, N.; Gerasopoulos, E. Field Evaluation of Low-Cost PM Sensors (Purple Air PA-II) Under Variable Urban Air Quality Conditions, in Greece. *Atmosphere* **2020**, *11*, 926.
- (18) Tryner, J.; L'Orange, C.; Mehaffy, J.; Miller-Lionberg, D.; Hofstetter, J. C.; Wilson, A.; Volckens, J. Laboratory Evaluation of Low-Cost PurpleAir PM Monitors and in-Field Correction Using Co-located Portable Filter Samplers. *Atmos. Environ.* **2020**, *220*, No. 117067.
- (19) Amouzouvi, Y. M.; Dzagli, M. M.; Sagna, K.; Török, Z.; Roba, C. A.; Mereuță, A.; Ozunu, A.; Edjame, K. S. Evaluation of Pollutants Along the National Road N2 in Togo Using the AERMOD Dispersion Model. *J. Health Pollut.* **2020**, *10*, No. 200908.
- (20) Diallo, A.; Hayaka, A.; Dossou-Yovo, K.; Assih, M.; Badjabaissi, E.; Ketoh, K. Étude de l'impact de la qualité de l'air sur la santé respiratoire des populations à Lomé (Togo). *Toxicol. Anal. Clin.* **2020**, *32*, 120–126.
- (21) Knippertz, P.; Fink, A. H.; Deroubaix, A.; Morris, E.; Tocquer, F.; Evans, M. J.; Flamant, C.; Gaetani, M.; Lavaysse, C.; Mari, C.; Marsham, J. H.; Meynadier, R.; Affo-Dogo, A.; Bahaga, T.; Brosse, F.; Deetz, K.; Guebsi, R.; Latifou, I.; Maranan, M.; Rosenberg, P. D.; Schlueter, A. A Meteorological and Chemical Overview of the DACCWA Field Campaign in West Africa in June–July 2016. *Atmos. Chem. Phys.* **2017**, *17*, 10893–10918.
- (22) Zodzi, J.; Prentice, A.; Gareth, J. Togo Revises up 2021 GDP Forecast to 5.3% *Reuters* Oct 7 2021.
- (23) Ouimette, J. R.; Malm, W. C.; Schichtel, B. A.; Sheridan, P. J.; Andrews, E.; Ogren, J. A.; Arnott, W. P. Evaluating the PurpleAir Monitor as an Aerosol Light Scattering Instrument. *Atmos. Meas. Tech. Discuss.* **2021**, 1–35.
- (24) Jayaratne, R.; Liu, X.; Thai, P.; Dumbabin, M.; Morawska, L. The Influence of Humidity on the Performance of a Low-Cost Air Particle Mass Sensor and the Effect of Atmospheric Fog. *Atmos. Meas. Tech.* **2018**, *11*, 4883–4890.
- (25) Magi, B. I.; Cupini, C.; Francis, J.; Green, M.; Hauser, C. Evaluation of PM<sub>2.5</sub> Measured in an Urban Setting Using a Low-Cost Optical Particle Counter and a Federal Equivalent Method Beta Attenuation Monitor. *Aerosol Sci. Technol.* **2020**, *54*, 147–159.
- (26) Giordano, M. R.; Malings, C.; Pandis, S. N.; Presto, A. A.; McNeill, V. F.; Westervelt, D. M.; Beekmann, M.; Subramanian, R. From Low-Cost Sensors to High-Quality Data: A Summary of Challenges and Best Practices for Effectively Calibrating Low-Cost Particulate Matter Mass Sensors. *J. Aerosol Sci.* **2021**, *158*, No. 105833.
- (27) McFarlane, C.; Raheja, G.; Malings, C.; Appoh, E. K. E.; Hughes, A. F.; Westervelt, D. M. Application of Gaussian Mixture Regression for the Correction of Low Cost PM<sub>2.5</sub> Monitoring Data in Accra, Ghana. *ACS Earth Space Chem.* **2021**, *5*, 2268–2279.
- (28) Crilley, L. R.; Shaw, M.; Pound, R.; Kramer, L. J.; Price, R.; Young, S.; Lewis, A. C.; Pope, F. D. Evaluation of a Low-Cost Optical Particle Counter (Alphasense OPC-N2) for Ambient Air Monitoring. *Atmos. Meas. Tech.* **2018**, *11*, 709–720.
- (29) Baron, R.; Saffell, J. Amperometric Gas Sensors as a Low Cost Emerging Technology Platform for Air Quality Monitoring Applications: A Review. *ACS Sens.* **2017**, *2*, 1553–1566.
- (30) Wang, Y.; Du, Y.; Wang, J.; Li, T. Calibration of a Low-Cost PM<sub>2.5</sub> Monitor Using a Random Forest Model. *Environ. Int.* **2019**, *133*, No. 105161.
- (31) Hagler, G. S. W.; Williams, R.; Papapostolou, V.; Polidori, A. Air Quality Sensors and Data Adjustment Algorithms: When Is It No Longer a Measurement? *Environ. Sci. Technol.* **2018**, *52*, 5530–5531.
- (32) Nowack, P.; Konstantinovskiy, L.; Gardiner, H.; Cant, J. *Towards Low-Cost and High-Performance Air Pollution Measurements using Machine Learning Calibration Techniques*; preprint; Gases/In Situ Measurement/Data Processing and Information Retrieval, 2020. DOI: 10.5194/amt-2020-473.
- (33) Marais, E. A.; Wiedinmyer, C. Air Quality Impact of Diffuse and Inefficient Combustion Emissions in Africa (DICE-Africa). *Environ. Sci. Technol.* **2016**, *50*, 10739–10745.
- (34) Schuster, G.; Dubovik, O.; Holben, B. N. Angstrom Exponent and Bimodal Aerosol Size Distributions. *J. Geophys. Res.: Atmos.* **2006**, *111*, No. D07207.
- (35) Magnoudéwa, B. B. Rapport Sectoriel D' Inventaire Des Gaz A Effet De Serre Du Togo. Laboratoire GTVD Gestion, Traitement et Valorisation des Déchets Université de Lomé, April 2021.

(36) Mudu, P. *Ambient Air Pollution and Health in Accra*; WHO Urban Health Initiative: Ghana, 2021.

(37) Gnamien, S.; Yoboué, V.; Liousse, C.; Osohou, M.; Keita, S.; Bahino, J.; Siélé, S.; Diaby, L. Particulate Pollution in Korhogo and Abidjan (Cote d'Ivoire) during the Dry Season. *Aerosol Air Qual. Res.* **2021**, *21*, No. 200201.

(38) Audu, V. E. M. Determination of Air Pollution Due to Traffic in Kaduna Town, (Kasuwa, Kawo Motor Park and Sabo) Kaduna State-Nigeria. *Int. J. Eng. Res.* **2018**, *V7*, 250–253.